Post-Dryout Heat Transfer in Tubes with Uniform and Circumferentially Nonuniform Heating

F. MAYINGER and R. SCHNITTGER

Measurements of wall temperatures under post-dryout conditions with uniformly and non-uniformly heated tubes in the refrigerant R12 are presented. Supplementary to these measurements a semi-empirical model was developed which predicts the temperatures of the wall and of the superheated vapour and the real quality downstream of the dryout spot.

Using the model one has to perform a stepwise numerical integration along the flow path of the droplet-vapour mixture, starting from the dryout spot. The basic idea of the model is the assumption that droplets are splitted into smaller particles under the influence of the shear stress in the boundary layer at the wall and during dry collisions with the wall.

Measured and predicted data are compared and give good agreement for uniformly heated tubes, and a satisfactory one for nonuniform heating. A comparison with data from the literature measured in water, proves that the model is also valid for this substance.

1. INTRODUCTION

For designing steam generators and for selecting the material of its tubes the exact knowledge of the wall temperatures to be expected is of high importance. Once-through steam generators - for example of the Benson type - have a heat transfer area where the cooling of the tube walls is produced by a dispersed flow with droplets embedded in vapour and with wall temperatures above wetting conditions. This situation is called post-dryout heat transfer.

The dryout of the wall is caused by two different phenomena: Evaporation reduces the thickness of the liquid film existing before at the wall and also the entrainment of droplets by the momentum forces resulting from the vapour flow decreases the amount of liquid at the wall. Mechanisms of this droplet formation are described for example by Hewitt [1], Langner [2] and Mayinger [3]. A large number of correlations exist to predict the onset of dryout, see for example [1] and [4-9]. In designing the thermohydraulic behaviour of Benson-boilers being operated at subcritical pressures frequently the dryout correlations by Bertoletti [9] or by Konkov [4] are used.

In the post-dryout region the heat transport from the tube wall can be subdivided into the following paths:

a) Convective heat transfer from the tube wall to the vapour,

b) heat transfer from the wall to droplets impinging on to the wall by radial movement in the boundary layer, however, not wetting the wall (dry collisions),

c) heat transfer from the wall to droplets wetting the wall for a short time (wet collisions),

d) heat transfer by radiation from the wall to vapour and droplets.

The contribution of these heat transfer paths were studied in detail by Hoeje [10]. One of his important findings was that the heat transport by wetting droplets becomes negligible small at wall temperatures 80 K above saturation temperature. Also the significance of dry collisions is strongly reduced with increasing vapour quality. So the main mechanism is the heat transfer from the wall to the vapour, which is super-heated, and from which - as a consequence - a thermodynamic non-equilibrium between vapour and droplets originates. A measure for this non-equilibrium is the ratio of the real quality $\dot{x}_{tat}$ and the quality $x_{G,g}$ which would exist if thermodynamic equilibrium would be present, that is, if the vapour would not be superheated or would have given all this superheating to evaporate droplets.

$$\frac{\dot{x}_{tat}}{x_{Gg}} = \frac{r}{h_{D,tat} - h_{F1,s}} \qquad (1)$$

In this equation r stands for the latent heat of vaporization and $(h_{D,tat}-h_{F1,s})$ is the difference between the real enthalpy of the vapour (D) and the enthalpy of the saturated liquid (F1). Radiation usually can be neglected with the tube diameters used in boilers.

In the literature there is a large number of measurements and correlations presenting the heat transfer in vertical tubes [11-20]. The correlations can be subdivided into the following categories:

1. Empirical correlations assuming thermodynamic equilibrium between the phases.

2. Correlations considering the thermodynamic non-equilibrium by empirical factors.

3. Semi-theoretical, non-equilibrium models calculating the heat transport stepwise.

A correlation belonging to the second category, for example, was presented by Groeneveld and Delorme [21]. Plummer [22] developed a two-step correlation and newer models were presented, for example, by Ganic and Rohsenow [23 and Chen [24].

2. DELIBERATIONS TO PREDICT POST-DRYOUT HEAT TRANSFER

A new model, which upto now is only presented in the Ph.D. - thesis of one of the authors [25], was developed by Schnittger. According to Fig.1 the following energy balance can be established for a steady state, one-dimensional dispersed flow:

$$d\dot{Q} + \dot{M}_D \cdot h_{D.tat} + \dot{M}_{Tr} \cdot h_{Tr} - [\dot{M}_D \cdot h_{D.tat} + d(\dot{M}_d \cdot h_{D.tat})] - [\dot{M}_{Tr} \cdot h_{Tr} + d(\dot{M}_{Tr} \cdot h_{Tr})] = 0 \quad (2)$$

The abbreviations and especially the indices in this equation and in the following ones are explained in the nomenclature.

The heat added to the dispersed system results from the heat flux density $\dot{q}$ at the wall.

$$dQ = \dot{q} \cdot \pi \cdot D_i \cdot dL \quad (3)$$

With the definition $M_D = M_{ges} \cdot x_{tat}$ and by substituting Equ.(3) in Equ.(2) one can write

$$\dot{q} \pi D_i = \underbrace{\dot{M}_{ges} (h_{D,tat} - h_{F1,s}) \frac{d\dot{x}_{tat}}{dL}}_{\text{Term 1}} + \underbrace{\dot{M}_{ges} \dot{X}_{tat} \frac{dh_D}{dL}}_{\text{Term 2}} \quad (4)$$

In this equation the first term on the right side gives the increase of vapour quality due to droplet evaporation and the energy needed to heat up the newly produced vapour from the saturation temperature to the real superheated temperature. In term 2 the enthalpy-rise of the vapour, due to additional superheating from the wall, is presented.

The increase of vapour quality, which would occur if thermodynamic equilibrium would exist, can be calculated from a simple energy balance:

$$dX_{G,g} = \frac{q \cdot \pi \cdot D_i}{\dot{M}_{ges} \cdot r} dL \quad (5)$$

The change of the real vapour quality is only depending on the heat additions $d\dot{Q}_{Tr}$ to the droplets

$$d\dot{X}_{tat} = \frac{d\dot{Q}_{Tr}}{\dot{M}_{ges} \cdot r} \quad (6)$$

Re-arranging the Equs. (4), (5) and (6) we get the differential equation

$$\frac{dh_{D,tat}}{dL} = \left(\frac{d\dot{x}_{G,g}}{dL} - \frac{h_{D,tat} - h_{F1,s}}{r} \frac{d\dot{Q}_{Tr}}{\dot{M}_{ges} \cdot r \cdot dL} \right) \frac{r}{\dot{X}_{tat}} \quad (7)$$

describing the change of vapour enthalpy $h_{D,tat}$ along the flow path in the tube, starting from the spot where the dryout occurs. At this spot we assume - as starting conditions for the integration - thermodynamic equilibrium between the droplets and the vapour. However, to start this integration we have to know the heat transfer between the vapour and the droplets, and the heat transfer from the wall to the vapour. For the latter one we can use the equation by Groeneveld-Delorme:

$$\alpha_D = \frac{q}{T_w - T_{D,tat}} = \frac{\lambda_f}{D_i} 0.008348 \left[\frac{m \ Di}{\eta_f} \left(\dot{X}_{tat} + \frac{g_{D,tat}}{g_{Fl}} (1 - \dot{X}_{tat}) S \right) \right]^{0.8774} Pr_f^{0.6112} \quad (8)$$

The real vapour quality $\dot{x}_{tat}$ we can express by re-arranging Equ. (1) with the differential superheating $dh_{D,tat}$ of the vapour, starting from the dryout spot

$$\frac{\dot{X}_{tat}}{\dot{X}_{G\,g}} = \frac{r}{h_{D,Do} + dh_{D,tat} - h_{Fl,s}} \quad (9)$$

The thermodynamic properties in Equ.(8) have to be selected at the reference temperature T_f

$$T_f = \frac{T_W + T_{D,tat}}{2} \quad (10)$$

We have now to discuss the heat transport dQ_{Tr} before we can integrate Equ.(7):

The heat transport between the superheated vapour and the droplets can be treated similarly to that between a small sphere and a gas flow, however, with a correction for the saturated vapour cushion around the liquid droplet.

Such a correction was proposed by Hoffmann and Ross [26] by using the Spalding-number B

$$B = \frac{h_{D,tat} - h_{D,s}}{r} \quad (11)$$

Doing this, one gets for the heat transfer coefficient at the vapour-droplet interface the equation

$$\alpha_{Tr} = \frac{\lambda_{D,f}}{D_{Tr}} (2 + 0.459 \cdot Re_{Tr}^{0.55} \cdot Pr_f^{0.33}) \cdot (1 + B)^{-0.6} \quad (12)$$

with the definition for the droplet-Reynolds-number Re_{Tr}

$$Re_{Tr} = \frac{D_{Tr} \cdot g_D \cdot W_{rel}}{\eta_D} \quad (13)$$

For small droplets following the vapour flow without slip we can simplify Equ.(12)

$$\alpha_{Tr} = \frac{\lambda_{D,f}}{D_{Tr}} \cdot 2 \cdot \left(\frac{1}{1 + B} \right)^{0.6} \quad (12a)$$

The total heat transported to the droplets in the tube section dL then reads

$$d\dot{Q}_{Tr} = \alpha_{Tr} \ N \ \pi \ D_{Tr}^2 \ (T_{D,tat} - T_s) = \frac{2 \cdot \lambda_{D,f} \cdot N \cdot D_{Tr}}{(1 - B)^{0.6}} \cdot (T_{D,tat} - T_s) \quad (14)$$

with N representing the number of droplets existing in this tube section. From the droplet flow N.

$$\dot{N} = \frac{\dot{M} \cdot (1 - \dot{x})}{\pi/6 \cdot D_{Tr}^3 \cdot g_{F1}} \quad (15)$$

and with the assumption that the droplets have the same velocity as the vapour we get

$$N = \frac{\dot{N}}{w_D} \, dL \quad (16)$$

substituting the vapour velocity in Equ.(16) and introducing it in Equ.(14) we find

$$d\dot{Q}_{Tr} = \frac{3 \cdot \lambda_{D,f} \cdot D_i^2 \cdot (1 - \dot{x}_{tat}) \cdot g_D \cdot dL}{(1 - B)^{0.6} \cdot D_{Tr}^2 \cdot g_{F1}} (T_{D,tat} - T_s) \quad (17)$$

we now need a correlation for the mean droplet diameter D_{Tr} at the dryout spot, because the integration of Equ.(7) has to start there. Measurements of droplet diameters are, for example, presented in [2] and [27]. Using these data, and based on a dimensionless analysis, the following empirical correlation was developed for the mean droplet diameter [25] at the dryout spot:

$$D_{Tr,Do} = 683.5 \cdot \frac{\eta_D}{w_{Do} \cdot \rho_D} \cdot \left(\frac{\sigma}{w_{Do} \cdot \eta_{F1}}\right)^{0.4} \left(\frac{1 - \dot{x}_{Do}}{\dot{x}_{Do}}\right)^{0.25} \cdot \left(\frac{\rho_{F1}}{\rho_D}\right)^{0.325} \cdot \left(\frac{\eta_D}{\eta_{F1}}\right)^{0.1} \quad (18)$$

In this equation the dimensionless group $\sigma/w_{Do}\,\eta_{F1}$ represents the ratio between the surface tension acting on a droplet departing from the liquid film at the dryout spot and the shear stress, due to vapour flow at the same place. The velocity w_{Do} of the vapour at the dryout spot can be calculated with the mass flow rate density $\dot{m} = \dot{M}/A$ of the mixture:

$$w_{Do} = \frac{\dot{m} \cdot \dot{x}_{Do}}{g_D} \quad (19)$$

Principally, we could now start to integrate Equ.(7) which, however, would comprise the assumption that the number of droplets along the flow path through the tube remains constant, unless they disappear due to total evaporation. Comparing results, calculated this way with measured data, we would realize that the correlation predicts too high wall temperatures or too low heat transfer coefficients, respectively. Therefore, an additional physical phenomenon obviously has to be taken into account. One can think about different possibilities of an incorrect description of the fluid dynamic behaviour in the above mentioned calculating procedure. So the mean droplet diameter may not be chosen correctly, or the assumption that the droplets have the same velocity as the vapour may be too conservative. However, attempts to fit the calculated data to the measured ones by corrections of that kind would bring the theoretical and experimental results into line only within narrow regions, but not over the full length of the tube where post-dryout heat transfer is present, and also for a limited set of parameters only.

So the idea came up that the droplets may undergo an alteration on its way to the tube. Droplets travelling near the wall can have dry collisions with the wall and, due to the steep velocity profile in the boundary layer, are subjected to a higher shear stress than in the center of the flow. Both phenomena may result in a splitting of a droplet into two or several liquid particles. Larger droplets may lose its spherical form.

In addition, a droplet in the boundary layer near the wall is surrounded by a vapour of higher temperature than in the center of the tube. Even without wetting, dry collisions produce a higher momentary evaporation rate than during the transport of the droplets in the core of the superheated vapour.

Schnittger [25] performed detailed deliberations on different effects acting onto the droplets in the boundary layer near the wall and he came out with a semi-empirical correlation which takes into account the increase of the number of droplets and the decrease of the mean droplet diameter, due to droplet splitting by dry collisions and flow-shear stress. He gave the equation for the change in droplet flow rate $d\dot{N}$ versus the differential flow path dL

$$d\dot{N} = K_1 \cdot \dot{N} \left(\frac{\dot{N}}{\dot{N}_{Do}}\right)^{k_4} \cdot \left(\frac{D_{Tr}}{D_i}\right)^{k_2} \cdot Re_D^{k_3} \cdot \frac{1}{D_i} \cdot \left(\frac{\pi/6 \cdot D_{Tr}^3 \cdot g_{Tr}}{\pi/6 \cdot D_{Tr,max}^3 \cdot g_{Tr}} - 1\right) \cdot dL \quad (20)$$

The maximum droplet diameter

$$D_{Tr,max} = \frac{\sigma \cdot We_{krit}}{\Delta w^2 \cdot g_D} \quad (21)$$

is calculated with the critical Weber-number

$$We_{krit} = \frac{D_{Tr} \cdot g_D \cdot w_{rel}^2}{\sigma} = 4.5 \div 21 \quad (22)$$

Integrating Equ.(20) we get

$$\int_{\dot{N}_1}^{\dot{N}_2} \frac{d\dot{N}}{\dot{N}^{(1+k_4)}} = \int_0^{\Delta L} k_1 \left(\frac{1}{\dot{N}_{Do}}\right)^{k_4} \cdot \left(\frac{D_{Tr}}{D_i}\right)^{k_2} \cdot Re_D^{k_3} \cdot \frac{1}{D_i} \cdot \left(\frac{\pi/6 \cdot D_{Tr}^3 \cdot g_{Tr}}{\pi/6 \cdot D_{Tr,max}^3 \cdot g_{Tr}} - 1\right) \cdot dL \quad (23)$$

In a stepwise numerical integration, starting from the dryout spot, we now can define $\dot{N}_1$ as the droplet flow rate at the entrance, and $\dot{N}_2$ as the droplet flow rate at the outlet of the tube section dL. We then can re-write Equ.(23) and get

$$N_2 = \left(N_1^{-0.3} - 8.4 \cdot 10^{-7} \left(\frac{1}{\dot{N}_{Do}}\right)^{0.3} \left(\frac{D_{Tr}}{D_i}\right) \cdot Re_D^{0.3} \cdot \frac{1}{D_i} \cdot \left(\frac{\pi/6}{\pi/6} \cdot \frac{D_{Tr}^3 \cdot \rho_{Tr}}{D_{Tr,max}^3 \cdot \rho_{Tr}} - 1\right) \cdot \Delta L\right)^{-\frac{1}{0.3}} \quad (24)$$

For the critical Weber-number in Equ.(21) a value of 7.5was derived from measurements. Combining Equs.(7), (12a), (14), (15) and (24), we can now perform a stepwise integration along the flow path through the tube in the post-dryout region and get the real vapour quality and the temperature of the superheated vapour. Returning then to Equ.(8) and by using the well-known interrelation

$$q = \alpha (T_W - T_s) = \frac{Nu\lambda_D}{Di} (T_W - T_s) \qquad (25)$$

we can predict the wall temperature T_w.

3. EXPERIMENTAL TECHNIQUES

Measurements of heat transfer under post-dryout conditions were performed with the refrigerant R12 in 6.12 m long tubes of 12.5 and 24.3 mm inner diameter. The principal arrangement of the experimental apparatus is shown if Fig.2.

The test section itself - the cylindrical tube - was equipped with several thermocouples measuring the wall temperature along the flow path. The real temperature of the superheated vapour in the test section was measured with a special thermocouple arrangement according to Nijhawan [28], which guaranteed that the welding of the thermocouple was only exposed to superheated vapour, but not to liquid droplets. The design of the thermocouple arrangement is shown in Fig.3.

For uniform heating the tube wall served as ohmic resistance. With non-uniform heating over the circumference of the tubes the heat addition was a little more difficult. As shown in Fig.4, an arrangement of indirect heating was chosen. Heating elements were pressed onto the upper half of the outer tube surface by means of an insulating material and a clamp. Each of the heating elements produced the same heat flux so that the heat addition was constant over the half perimeter of the tube within a certain waviness. The tubes had a wall thickness of 2.5 and 4.5 mm respectively, depending on the tube diameter. Therefore, a certain amount of heat can be tangentially transported by conduction in the tube wall, flattening the circumferential power profile. The tangential heat transport is a function of the thermal conductivity of the tube material and of the heat transfer coefficient on the cooled side of the tube.

4. COMPARISON OF MEASURED AND CALCULATED DATA

Measurements were performed with the refrigerant R12 at pressures between 10 and 28 bar, with mass flow rate densities from 400 to 2400 kg/m^{2}s, and with the heat flux densities between 1 and 6 W/cm^2. The experimental results are reported in [25] and [29] in detail. Most of the measurements were performed with uniformly heated tubes, however a part of the investigations was also aimed to see what influence circumferentially non-uniform heating has on the heat transport and whether the opposite cold wall reduces the temperature of the hot side.

Here, only comparisons between measured and calculated data shall be given. Boiler manufacturers are usually not interested in the heat transfer coefficient itself but more in the maximum wall temperature to be expected, because its value limits the design of the steam generating system. Therefore, wall temperatures will be reported here, instead of heat transfer coefficients. The latter comprises also the question of defining the vapour temperature. For practical use and to avoid unnecessary difficulties, it is recommended to choose the saturation temperature of the two-phase mixture - liquid droplets and vapour - in the well-known formulation $\dot{q} = \alpha (T_w - T_{D,s})$.

4.1 Uniformly heated tubes

The post-dryout heat transfer and, by this, the wall temperature of steam generator tubes are influenced by the heat flux and the mass flow rate density of the two-phase mixture, mainly. The tube diameter plays a minor role. Due to the varying density ratio between vapour and liquid the radial transportation of the droplets is depending on the pressure which, therefore, influences the cooling of the wall, too. A much stronger effect has the concentration of droplets in the mixture, however. Low quality, which means a high droplet concentration, guarantees a lower grade of thermodynamic non-equilibrium between the phases than high qualities, because the heat exchanging area between vapour and liquid and the thermal capacity of the liquid phase are larger. Low quality leads to a higher deposition rate of droplets into the superheated boundary layer near the wall. In the following, mainly the influences of the quality $\dot{x}$ and of the heat flux on the wall temperature will be discussed and the agreement between calculation and experiment examined.

The post-dryout heat transfer behaviour is not only quantitatively but also qualitatively different at high and at low qualities. At high qualities with low droplet concentration in the superheated vapour the wall temperature is continuously increasing behind the dryout spot along the flow path of the mixture, as Fig.5 shows. With low qualities, however, the heat transfer downstream of the dryout spot can even improve again, due to strong evaporation of the liquid, as demonstrated in Fig.7. This evaporation enlarges the specific volume of the mixture and, by this, the mean velocity is increased, which again favours the heat transport from the wall. The deposition rate at low qualities - Fig.7 - is much larger than at high qualities (Fig.5).

Both figures (5 and 7) also convey an impression how measured and semi-theoretically predicted wall temperatures agree. The semi-theoretical model, based on the assumption of droplet-splitting and dispersion, fits the experimental data especially in the low quality region, where droplet interaction with the boundary layer near the wall is dominant.

In both figures the temperatures on the inner side of the tube - the wall temperature - is plotted versus the flow path - the length of the tube - with

the heat flux as parameter. As discussed in chapter 3, the real vapour temperature $T_{D,sat}$ was measured by a thermocouple, which had a special protection against impinging droplets. The real vapour temperatures, corresponding to the thermo- and fluid dynamic parameters of Fig.5, are presented in Fig.6.

From the measured vapour temperature one can calculate - by a simple energy balance - the real vapour quality, which is also plotted in Fig.6. Comparisions of these experimentally gained data - real vapour temperature and, derived from that, real quality - with predicted ones by the semi-theoretical model give satisfactory agreement.

The tube diameter has a negligible small influence on the heat transfer under post-dryout conditions, as mentioned before and as a comparison of Figs.7 and 8 demonstrates.

The thermo- and fluid dynamic conditions of the experiments reported in these figures were similar, but the tube diameter in Fig.8 is twice of that in Fig.7. The degree of heat-transfer-enhancement downstream of the dryout spot is more and more marked with decreasing steam quality.

To prove that the model presented in chapter 2 is not only valid for the refrigerants but also for water, which is the usual working fluid in power engineering, comparisons were also made with experiments by Kastner [30]. The test section used by Kastner had the same dimensions as that in the R12 - loop presented here. An example of the agreement between correlated and measured data [30] is presented in Fig.9.

Scaling the thermodynamic properties between R 12 and water with the reduced pressure p/p critical, the pressure of 150 bar in the water-data of Fig.9 corresponds to the pressure of 27,9 bar in the R12-data of Fig.7. Comparing these two figures, one realizes with water an even more strongly marked enhancement of the heat transfer downstream of the dryout spot, which can be explained by the larger latent heat of vaporisation in water compared to R12. A more detailed analysis of the semi-empirical correlation with respect to its validity in water is presented in [29].

4.2 Circumferentially non-uniformly heated tubes

In a first evaluation of the data measured in tubes which were only heated from one side, as described in chapter 3, it was assumed that the circumferential heat conduction in the material of the tube wall can be neglected. This means that one half of the tube is uniformly heated and the opposite half would be unheated. Under dryout conditions the temperature of this unheated wall corresponds roughly to the temperature of the superheated vapour. Due to the limited number of heating elements - as described in chapter 3 - the temperature at the inner surface of the heated side of the tube shows a certain waviness, as shown in Fig.10.

In the graphs of the following figures this waviness is smoothed out.

The course of the wall temperatures on the heated and the unheated side of the tube is parallel along the flow path downstream of the dryout spot, as one can see from Fig.11.

This parallelism - but not the temperature difference - is independent from the heat flux. At low vapour qualities the grade of heat transfer enhancement was much smaller with non-uniform heating than it was observed with the uniformly heated tubes before. In this connection, however, it has to be mentioned that the dryout occurred under non-uniform heating conditions much later than under uniform ones at the same thermo- and fluid dynamic conditions. The downstream - shifting of the dryout spot - due to non-uniform heating - can be upto 1 m, as shown in Fig.12.

From this figure we also can see that the wall temperature on the heated side is lower with non-uniform heating than with the uniform one. This is caused by a better cooling, which again is a function of re-distribution of droplets in the vapour.

Finally, an attempt was made to predict the wall temperature under conditions of non-uniform heating with the same semi-empirical model - described in chapter 2 - as for uniform heating.

Fig.13 gives some information about the agreement or disagreement between measured and calculated data. The calculation always over-predicts the wall temperatures of the heated side in this case which, however, easily can be explained by the fact that in these calculations the circumferential heat conduction in the material of the tube wall was not yet taken in to account. Therefore, the over-prediction is larger with high heat fluxes. At low heat fluxes the circumferential heat conduction becomes negligible and then the calculated and measured data agree well. Therefore, the conclusion may be allowed that the semi-empirical model can also be used for non-uniformly heated tubes ; however, it gives conservative data for the wall temperature.

ACKNOWLEDGEMENT

The authors wish to thank the Bundesminister fuer Forschung und Technologie (BMFT) for financially supporting the work reported here.

NOMENCLATURE

- A area
- B Spalding-numbe
- c_p Specific heat
- D diameter
- h specific enthalpy
- L length
- $\dot{m}$ mass flow rate density
- $\dot{M}$ mass flow rate
- N number of droplets
- $\dot{N}$ flow rate of droplets

Nu Nusselt-number
p pressure
Pr Prandtl-number
q heat flux density
Q heat flux
Re Reynolds-number
r latent heat of evaporation
t time
T temperature
V volume
w velocity
We Weber-number
$\dot{x}$ vapour quality
α heat transfer coefficient
ϵ local void fraction
η dynamic viscosity
λ heat conductivity
ρ density
σ surface tension

Indices

D," vapour
Do dryout
f film
Fl,' liquid
g gas
G.g equilibrium
ges total
i inner
krit critical
max maximum
rel relative
s saturated
tat real
Tr droplet
W wall

REFERENCES

1. Hewitt, G.F., Hall-Tayler, N.S., Annular two-phase flow, Pergamon Press (1970)

2. Langner, H., Untersuchungen des Entrainment-Verhaltens in stationären und transienten zweiphasigen Ringströmungen, Dissertation, TU-Hannover (1978)

3. Mayinger, F., Strömung und Warmeubergang in Gas-Flüssigkeits Gemischen, Springer-Verlag Wien-New York, (1982)

4. Konkov, A.S., Experimental study of the conditions under which heat exchange deteriorates when a steam-water mixture flows in a heated tube, Teploenergetika 13 (12), 53-57 (1966).

5. Cumo, M., Ferrari,G., and Urbani,C., Prediction of burn-out power with Freon up to the critical pressure, 27th Meeting ATI, Napoli, Sep. (1972)

6. Roko, K, Takitani, K. et al. Dryout characteristics at low mass velocities in a vertical straight tube of a steam generator, Proceedings 6th Int.Heat Trans. Conf. Toronto, (1978).

7. Levitan, L.L., et al., Teploenergetika, (1975) 1.

8. Cumo, M.,et al., On the limiting critical quality and the "deposition controlled" burnout, Com.Nat.-Energia Nucleare, RT ING (79)4

9. Bertoletti, S., et al., Heat transfer crisis with steam-water mixtures, Energia Nucleare 12, (1956) 121.

10. Iloeje, O.C., Three step model of dispersed flow heat transfer, General Electric Presentation Post CHF Heat Transfer, Oct. (1975)

11. Miropolski, Z.L., Heat transfer in film boiling of a steam-water mixture in generating tubes, Teploenergetica, No.10, 5 (1963) 49-53.

12. Dougall, and Rohsenow, W.M., Film boiling on the inside of vertical tubes with upward flow of the fluid at low qualities, Techn· al Rep.No.9079-26 M.I.T. Dep. of Mech. Engineeri

13. Bishop, A.A., et al., Forced convection heat transfer at high pressure after the critical heat flux, ASME 65-HT-31, (1965)

14. Herkenrath, H., and Mörk-Mörkenstein,P., Wärmeübergang an Wasserbei erzwungener Strömung im Druckbereich von 140-250 bar, EUR-3678d, (1967)

15. Hynek, S.J., Rohsenow, W.M., and Bergles, A.B., Forced convection dispersed flow film boiling, M.I.T. Heat Transfer Lab., Rep.No. DSR 70586-63, (1969)

16. Brevi, R., Cumo, M., et al., Post-dryout heat transfer with steam/water mixtures, Trans.Am.-Nucl.Soc.,12 (1969) 809-811.

17. Lee,D.H., Studies of heat transfer and pressure drop relevant to subcritical once-through evaporators, IAEA-SM-130/56, IAEA Symp.on Progress in Sodium-Cooled Fast reactor Engineering, Monaco (1970)

18. Tong, L , Film boiling heat transfer at low quality subcooled region, Proc.2nd Joint - USAEC-EURATOM Two-Phase Flow Meeting, Germantown, Rep. CONF 640507 (1964) 63.

19. Slaughterbeck, and Mattson, Statistical regression analysis of experimental data for flow film boiling heat transfer, ASME Publ. at the ASME-AIChE Heat Trans. Conf.Atlanta/Ga.,(1973)

20. Laverty,W.F., and Rohsenow, W.M., Film boiling of saturated nitrogen flowing in a vertical tube, ASME 65-WA/HT-26, (1965)

21. Groeneveld, D.C., and Delorme, G.G.J., Prediction of thermal non-equilibrium in the post-dryout regime, Nuclear Engng. and Design 36 (1976) 17-26, North Holland Publ. Company.

22. Plummer, D.N., Post critical heat transfer to flowing liquid in a vertical tube, Ph.D.-Thesis, MIT,(1974)

23. Ganic,E.N., and Rohsenow, W.M., Post critical heat flux heat transfer, Techn.Rep.No.82672-97, Mass.Inst.of Techn.,(1976)

24. Chen, J.C., Sundaram, R.K., and Ozynak, F.T., A phenomenological correlation for post-Chf heat transfer, NUREG 0237,(1977)

25. Schnittger, R., Untersuchungen zum Wärmeübergang bei vertikalen und horizontalen Rohrströmungen im Post-Dryout-Bereich, Dissertation, Univ.Hannover,(1982)

26. Hoffman, T.W., and Ross,L.L., A theoretical investigation of the effect of mass transfer on the heat transfer to an evaporating droplet, Int.J. Heat Mass Trans. 15 (1972) 599 - 617.

27. Ueda, T., Tanaka,H., and Koizumi,Y., Dryout of liquid film in high quality, R-113 upflow in a heated tube, Proc.Int.Heat Transfer Conf.(1978) Toronto/Canada

28. Niihawan,S., Chen, J.C., Sundaram, R.K., and London, E.J.,aMeasurements ofvapor superheat in post-critical-heat-flux boiling, J.of Heat Transfer, 102 , (1980) 465-470.

29. Mayinger, F.,Schnittger,R., and Scheidt, M.,Untersuchungen zum Wärmeübergang bei vertikaler und horizontaler Rohrstromung, AbschluBbericht BMFT Forschungsvorhaben ET 1412A, (1982)

30. Kastner, W., Köhler, W., Krätzer, W.,, and Hein, D., Wärmeübergang im Post-Dryout-Bereich in vertikalen und horizontalen Rohren bei gleichformiger Beheizung, KWU-AbschluBericht zum-Forderungsvorhaben BMFT ET 1409A (1982)

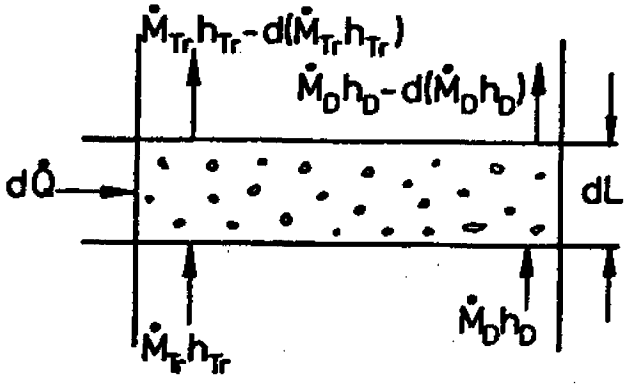

Fig.1 Energy balance of dispersed flow

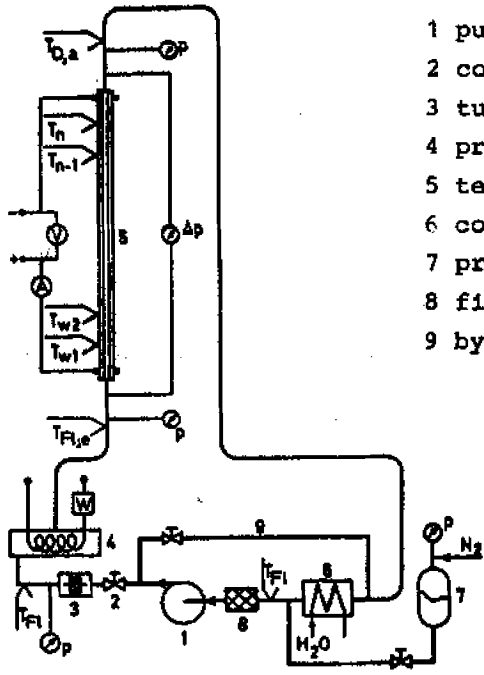

Fig.2 Test facility

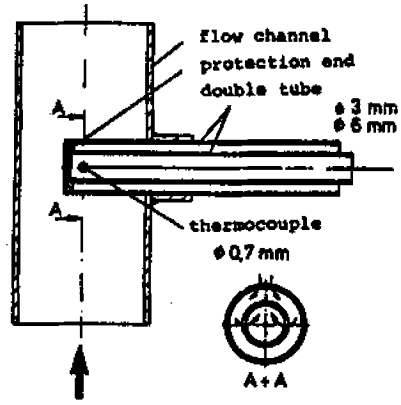

Fig.3 Thermocouple arrangement for superheated vapour in dispered flow

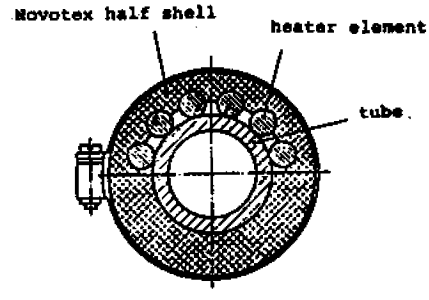

Fig.4 Heating elements on test tube

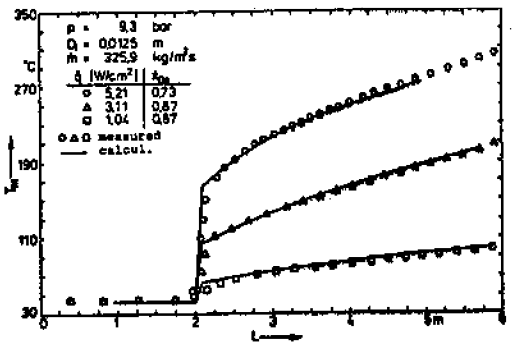

Fig.5 Comparison of measured and calculated wall temperatures with R12; high vapour qualities, no downstream enhancement

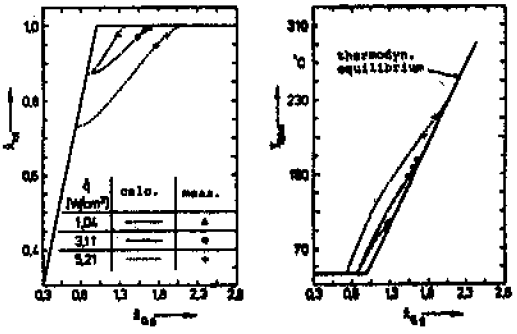

Fig.6 Real Vapour quality and temperatures of the superheated vapour as function of the fictitious equilibrium c equilibrium quality

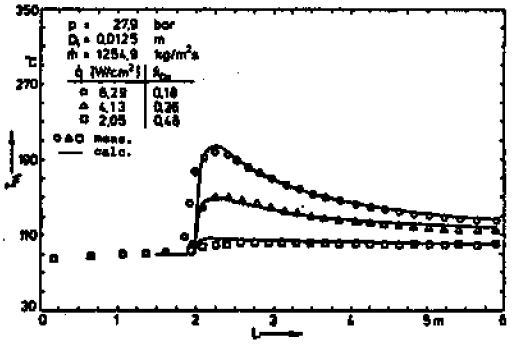

Fig.7 Wall temperatures with R12, low vapour qualities, downstream enhancement

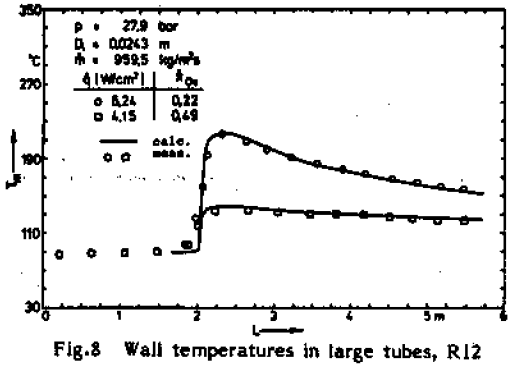

Fig.8 Wall temperatures in large tubes, R12